A study of the chemisorption of phenol and its derivatives on plasma-grown aluminium oxide by inelastic electron tunneling spectroscopy

I. W. N. McMorris, N. M. D. Brown, and D. G. Walmsley

Citation: The Journal of Chemical Physics **66**, 3952 (1977); doi: 10.1063/1.434446
View online: http://dx.doi.org/10.1063/1.434446
View Table of Contents: http://scitation.aip.org/content/aip/journal/jcp/66/9?ver=pdfcov
Published by the AIP Publishing

A study of the chemisorption of phenol and its derivatives on plasma-grown aluminium oxide by inelastic electron tunneling spectroscopy*

I. W. N. McMorris, N. M. D. Brown, and D. G. Walmsley

School of Physical Sciences, The New University of Ulster, Coleraine, Northern Ireland
(Received 5 April 1976)

Inelastic electron tunneling spectroscopy has been applied to study the adsorption of a series of phenols on plasma-grown aluminium oxide. Vapor phase doping was used and spectra recorded for *o*-, *m*-, *p*-chlorophenol, *p*-fluorophenol, *p*-bromophenol, *o*-, *m*-, *p*-cresol, and phenol. The high resolution spectra obtained at 2 K allow most of the possible modes to be identifield. The relative strengths of these modes are compared in terms of the proposed molecular orientation of the absorbates in an effort to observe the predicted directional sensitivity of the tunneling process. No systematic line intensity variation is evident, and it is postulated that for large molecules this may be because of the complexity of the motions involved in the vibrational modes. It is also suggested that the contouring of the lead electrode round the adsorbate has the important effect of obscuring the directional sensitivity of the tunneling process. An attempt has also been made further to characterize the chemical nature of the oxide and its surface.

I. INTRODUCTION

In 1966, Jaklevic and Lambe[1] related features in the current–voltage characteristic of metal–insulator–metal (MIM) tunnel junctions to the vibrational excitations of molecular impurities at the metal–insulator interface. These features they showed to be due to the inelastic tunneling of electrons; curves exhibiting them are known as inelastic electron tunneling (IET) spectra. Many have been published[2] for barrier oxide adsorbed organics, and quite a close correspondence with the infrared and Raman spectra of the same compounds has been noted.[2–7] In a number of cases, there is evidence for chemical reaction between adsorbate and oxide.

The present work systematically examines the possible use of IET spectroscopy to detect orientation of the adsorbate on the oxide surface. We have used a series of phenols because they undergo site-specific reaction and in addition are sufficiently volatile to allow vapor phase deposition. We propose the formation of a surface species in which symmetry of the parent molecule is retained. The spectra obtained from Al–I–Pb junctions exhibit good resolution, reproducibility, and very low levels of contamination. The availability of these high quality spectra has enabled us to identify all the important modes in the compounds studied and confirm the formation of a phenolate[6,7] anion on the oxide surface. We have examined the relative line intensities with a view to obtaining evidence for specific orientation of the adsorbate.

II. THEORETICAL CONSIDERATIONS

A. Dipole and induced dipole orientation

In developing a model for inelastic tunneling, Scalapino and Marcus[8] consider the case of an OH dipole at the interface between the oxide barrier and lead in an Al–I–Pb junction and show that the dipole moment (**P**) and its near image in the lead electrode combine to give only a dipole component ($2P_z$) perpendicular to the barrier. They assume that the insulator–lead interface is everywhere planar and then show that the additional contribution to the tunneling current for an electron–dipole interaction due to the inelastic process is

$$I_{\mathrm{INEL}} \propto \sum_m |\langle m|P_z|0\rangle|^2 .$$

Here $P_z = P_z^0 + z(dP_z^0/dz)$ and P_z^0 is the static dipole. Strictly, the image of the tunneling electron should also be considered and thus the total electric field seen by the dipole is in the z direction. The above matrix element may be expanded

$$\langle m|P_z|0\rangle = P_z^0\langle m|0\rangle + (dP_z^0/dz)\langle m|z|0\rangle ,$$

and it is known[9] that the first term vanishes unless $m=0$, the second term unless $m=\pm 1$. Hence a vibrational excitation occurs if $m=\pm 1$ and $dP_z/dz \neq 0$. The spatial rate of change of the z component of the electric dipole perpendicular to the barrier must be nonzero if a tunneling spectral line is to be observed.

Using the same model it can be shown[10] that for the electron induced–dipole case

$$I_{\mathrm{INEL}} \propto \sum_m |\langle m|\alpha|0\rangle|^2 ,$$

where α is the dipole polarizability tensor. Once again, it is only the net z component of the induced dipole moment which interacts with the field of the electron as any x- or y components will be cancelled by images in the lead electrode. Thus the only element of the polarizability tensor contributing to the inelastic current is α_{zz}, and by arguments similar to those above, a molecular excitation can be shown to occur only if $d\alpha_{zz}/dz \neq 0$ and $m=\pm 1$. The line intensities due to both processes should in principle have a high (viz. $\cos^2\theta$) orientation dependence. It should therefore be possible to deduce information about dipole orientation. Furthermore, it might seem possible in the more complex case of molecular adsorbates to obtain information on molecular orientation. Bogatina *et al.*[11] and Hansma[2] have already considered some spectra on this basis.

B. Top electrode shift

An oscillating electron dipole close to a plane metal surface suffers a drag due to interaction with its image.

The reduction in frequency has been shown by Antoniewicz[12] to be given by

$$\bar{\omega}_0^2 = \omega_0^2 - e^2/(4md^3) ,$$

where ω_0 is the natural frequency and $\bar{\omega}_0$ the shifted frequency.

Kirtley and Hansma[13,14] have found IET evidence to support the d^{-3} dependence of the shift on atomic radius of the top electrode metal. They report the largest shifts ($\simeq 15$ meV, 120 cm^{-1}) for OH stretch modes on the aluminium oxide.

C. Spectral line position correction

When one of the metal films in the tunnel sandwich becomes superconducting, the positions of all lines are shifted upward in energy by an amount equal to the superconducting energy gap of the film. The thermal smearing is reduced below that found when both metals are normal (5.44 kT) and the line shapes become asymmetrical.[10] Modulation of an asymmetric spectral line with amplitude comparable to its width leads to some distortion of shape and displacement of peak position of the detected signal. For the present analysis it is sufficient to know that the observed position of the spectral lines must be reduced by 1.00 mV (8.07 cm^{-1}) to correct for these effects. This has been done in recording data in the tables.

III. EXPERIMENTAL METHOD

A. Fabrication

Three Al–I–Pb junctions are made simultaneously on a glass microscope slide which is first carefully cleaned. Aluminium is evaporated from a multistranded tungsten filament to form a strip 60 mm long, 0.7 mm wide, and 1000 Å thick. A thin oxide is then grown in a dc plasma established in an oxygen atmosphere at a pressure of 0.03 Torr. A plasma current of 5 mA is maintained for a time (30–90 s) which varies with sample type. The organic vapor is introduced by opening the evacuated ($\simeq 10^{-6}$ Torr) evaporator chamber to a reservoir of liquid which is usually heated. A quartz crystal, located close to the slide, is used as a microbalance to monitor the amount of vapor deposited at the sample. During subsequent pumpdown much of that deposited is desorbed, but for the compounds discussed here a characteristic amount is found to remain for each. Finally the lead counter electrodes (0.7 mm wide, 7000 Å thick) are cross deposited from a molybdenum boat. Filaments and masks are changed whilst the system is under vacuum and the microscope slide remains *in situ* during all stages of sample preparation. The vacuum chamber is pumped by a diffusion pump operating with a very stable high boiling point oil, SANTOVAC 5, and in addition the backing line has a Zeolite trap.

Vapor doping suffers as a technique from two shortcomings: it cannot handle involatile compounds, and there is a great danger of cross contamination between successive compounds studied. The doping facility used here consists of a glass reservoir external to the main chamber and connected to it through a valved tube which feeds into the evaporator baseplate. Between doping with different compounds the whole doping facility is cleaned by stripping down, washing, and baking out. At the same time the main chamber is cleaned by heating with hot air blowers. A prolonged plasma discharge at high current is then usually run and an undoped test sample is prepared. If there is evidence of spectral lines due to organic contamination, the entire process is repeated until none are detected. Whilst this procedure may be time consuming, it is justified by the relatively contamination-free spectra obtained. Only after a spectrum of a particular adsorbate has been satisfactorily reproduced at least twice from independent fabrications is it regarded as of adequate quality.

All the phenols used were obtained from commercial sources. Prior to use they were vacuum distilled or sublimed, as appropriate, to a purity better than 99.5% as found by gas liquid chromatography.

Copper leads are attached to the samples with indium and the substrate is supported on a Tufnol bonded laminate holder suspended by a stainless steel tube. The assembly is cooled to 2 K in a standard double glass liquid helium cryostat.

B. Electronics

The circuit (see Fig. 1) is similar to that first used by Lambe and Jaklevic[10] and more recently by Lewis *et al.*[4] A 2.0 mV peak-to-peak sinusoidal voltage is applied (at 50 kHz) in parallel with the dc bias across the sample. The filter network discriminates strongly against development of the fundamental across the input of the signal detection amplifier by having an impedance matching transformer tuned to the second harmonic and developing the fundamental across a resonant loop. This improves the second harmonic to fundamental signal ratio at the input to the amplifier by at least 10^5 over that at the sample. An Ortec Brookdeal 9501 wide band lock-in amplifier acts as detector. The dc bias is provided by an electrically driven, geared potentiometer fed from rechargeable cells, and the total sweep time for a spectrum is usually about 1 h.

IV. RESULTS

Representative and typical examples of tunnel spectra of Al–I–Pb junctions doped with various phenols are shown in Figs. 2–6. Tables I–IV list the corrected

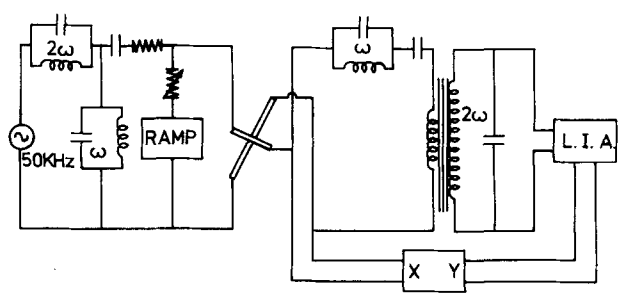

FIG. 1. A schematic diagram of the circuitry used for obtaining the second derivative, d^2V/dI^2.

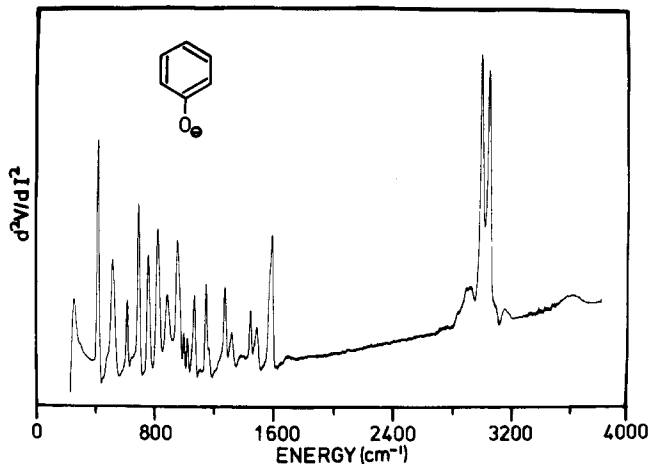

FIG. 2. A tunneling spectrum of phenolate anion at 2 K on plasma grown Al oxide; a modulation voltage $V_m = 2$ mV peak-to-peak was used.

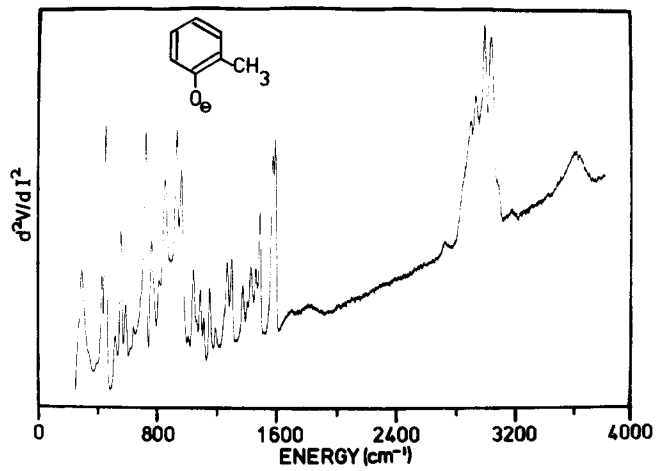

FIG. 4. A tunneling spectrum of o-cresolate anion at 2 K on plasma grown Al oxide, $V_m = 2$ mV p–p.

(see earlier) IETS line positions (1 cm^{-1} = 8065 meV) and the apparent line intensities. The latter are expressed simply as the ratio of the height of a given line to that of an arbitrarily chosen line (at $\simeq$400 cm^{-1}) which is set at unity. Apart from the few situations where lines overlap, most have comparable linewidths ($\simeq$ 20 cm^{-1}) at half-height under the chosen experimental conditions. These observed linewidths significantly exceed the calculated modulation and thermal smearing which would amount to only 9 cm^{-1}.

For purposes of comparison, the corresponding positions and assignments[15–21] of the vibrational fundamental modes of the various phenols used are also given in the tables. Dilute solution values are chosen since we consider these to be more appropriate than those of the bulk or nondilute phenols because of the isolated nature of the surface adsorbed species present in the tunnel junctions. Ideally, comparison should be made with the optical vibrational spectra of the adsorbent/adsorbate system (see later).

V. FUNDAMENTAL VIBRATIONS AND ASSIGNMENTS

A. Phenol and p-X-phenol (X = F, Cl, Br, and CH_3) modes

Phenol and the p-substituted phenols are considered to belong to the C_{2v} point group with the OH moiety and CH_3 group treated as point centers of mass lying on the C_2 axis, conventionally[22] the z axis of the molecule (which is not necessarily the z axis of the barrier). The yz plane is the plane of the molecule with the x axis perpendicular at the center of the six-membered ring. The 30 fundamentals are distributed $\Gamma = 11a_1 + 3a_2 + 6b_1 + 10b_2$. Apart from the a_2 modes which are Raman active only, the other 27 are both infrared and Raman active. For phenol, 24 vibrations are essentially independent of the OH group with the remaining six modes involving significant motion of the substituent. In addition there are the 3 modes of the OH group: ν(OH), δ(OH), and γ(OH) are, respectively, stretching, in-plane bend, and torsional in type. Table I details all 33 modes for phenol.[15–17]

Available vibrational data of the p-substituted phen-

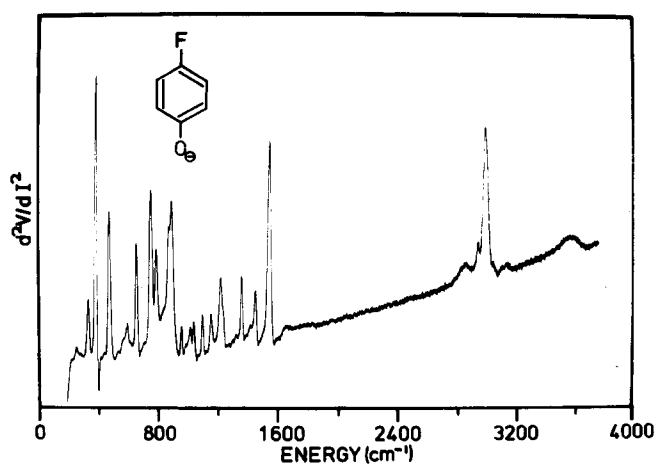

FIG. 3. A tunneling spectrum of p-fluorophenolate anion at 2 K on plasma grown Al oxide, $V_m = 2$ mV p–p.

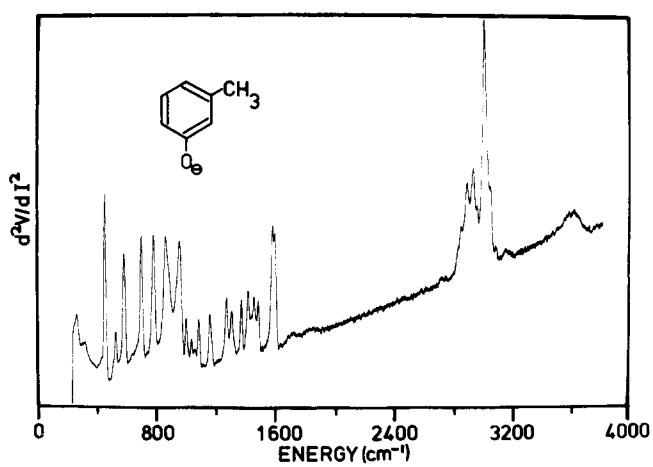

FIG. 5. A tunneling spectrum of m-cresolate anion at 2 K on plasma grown Al oxide, $V_m = 2$ mV p–p.

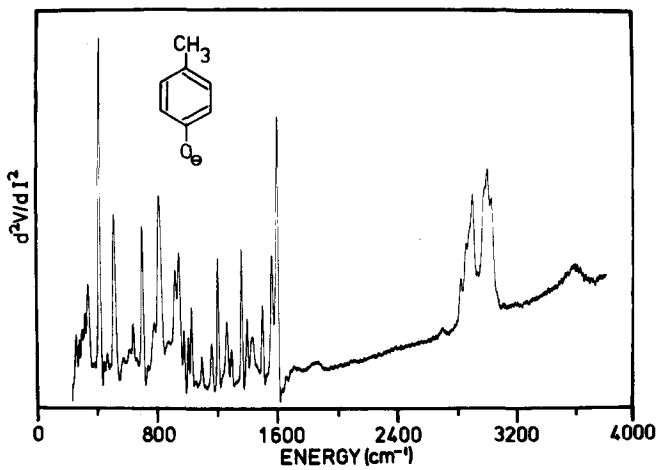

FIG. 6. A tunneling spectrum of *p*-cresolate anion at 2 K on plasma grown Al oxide, V_m = 2 mV p–p.

ols[15] and related *p*-substituted benzenes[18] show that some nine modes are substituent sensitive. See Table II. The CH_3 group modes are in Table IV.

B. *o*-X-phenols and *m*-X-phenol (X = Cl and CH_3) modes

The 30 fundamentals of these systems, again treating the OH and CH_3 groups as point masses, comprise $21a'$ and $9a''$ modes with C_s symmetry assumed. In addition there are the three OH modes ($2a'$ and $1a''$) and those of the CH_3 group. All are both infrared and Raman active. In the *o*-phenols, 11 of the 30 fundamentals are substituent sensitive,[15,19] as are 10 in the *m*-phenols.[15,20] These and the other modes are given in Table III along with the OH modes; the CH_3 group vibrations are in Table IV.

C. Assignments

In the tables, appropriate mode assignments have been made from the relevant literature. We recognize the difficulty in drawing precise conclusions about the details[23–26] of the nuclear motions involved. For example, the $a_1\nu_5$ and $a_1\nu_8$ or $b_2\nu_{24}$ and $b_2\nu_{28}$ modes of the phenolate could well be of quite mixed character[24] as will many of the others. However, for convenience and later discussion the nominal assignments are retained.

VI. DISCUSSION

A. Al oxide, surface reactivity, and general considerations

From the various tunnel spectra, it is immediately clear that the vibrational modes associated with the OH group of the phenols are absent. These changes are ascribed to reaction of the phenols with surface bound OH groups (Brönsted acid sites) and with cationic surface aluminium centers (Lewis acid sites) to form in either case chemisorbed phenolate ions. Such behavior is generally accepted for adsorbates on bulk aluminas and has been discussed previously in terms of both conventional infrared spectra[27,28] of adsorbed phenols and more recently in an IET study of surface adsorbed hydroxybenzenes.[7] It would therefore seem reasonable to say that the plasma grown oxide, at least in terms of its surface properties, behaves like bulk aluminas.

As many as five distinct OH environments have been distinguished in detailed studies[29–31] of the infrared spectra of variously heat treated γ aluminas in the OH stretching region (3500–3850 cm^{-1}). In these the actual position of the OH stretching mode is held to depend on

TABLE I. IETS Data of chemisorbed phenol on plasma grown aluminium oxide, i.e., the phenolate anion.

	Vibrational fundamentals in cm^{-1}			
IETS[a]	ir-Raman[b]	Symmetry class[c]	Mode diagram[d]	Approx. description[e]
	3085	ν_1	Z_1	ν(CH)
3036 (1.20)	3076	ν_2	Z_3	ν(CH)
2985 (1.12)	3044	ν_3	Z_4	ν(CH)
1583 (0.57)	1604	ν_4	k	ν(CC)
1482 (0.17)	1497	ν_5	m	ν(CC)
1269 (0.36)	1259	a_1 ν_6	q	ν(CO)
1159 (0.11)	1167	ν_7	a	β(CH)
1019 (0.13)	1026	ν_8	b	β(CH)
994 (0.13)	999	ν_9	p	ring
819 (0.25)	812	ν_{10}	r	X sensitive
511 (0.25)	526	ν_{11}	t	X sensitive
949 (0.21)	958	ν_{12}	h	γ(CH)
819 (0.25)	825	a_2 ν_{13}	g	γ(CH)
410 (0.50)	408	ν_{14}	w	ϕ(CC)
949 (0.21)	978	ν_{15}	j	γ(CH)
881 (0.22)	881	ν_{16}	i	γ(CH)
753 (0.50)	749	ν_{17}	f	γ(CH)
688 (0.72)	688	b_1 ν_{18}	v	ϕ(CC)
511 (0.25)	500	ν_{19}	y	X sensitive
247 (0.20)	241	ν_{20}	x	X sensitive
3036 (1.20)	3091	ν_{21}	Z_4	ν(CH)
2985 (1.12)	3030	ν_{22}	Z_5	ν(CH)
1565 (0.37)[f]	1596	ν_{23}	l	ν(CC)
1440 (0.23)	1465	ν_{24}	n	ν(CC)
... ...	1339	ν_{25}	o	ν(CC)
1314 (0.16)	1313	b_2 ν_{26}	e	β(CH)
1142 (0.39)	1145	ν_{27}	c	β(CH)
1064 (0.33)	1075	ν_{28}	d	β(CH)
615 (0.31)	617	ν_{29}	s	α(CCC)
410 (0.50)	408	ν_{30}	u	X sensitive
...	3600			ν(OH)
...	1175			δ(OH)
	310			γ(OH)

[a] As discussed in the text, the relative intensities shown in parentheses are arbitarily scaled with respect to the line at 410 cm^{-1} set to unity; where accidental line coincidences are believed to occur, the observed intensity is shared between the coincident modes.

[b] The line position data listed are of phenol in dilute solution, Refs. 15–17.

[c] C_{2v} point group with the recommedned choice of coordinates, Ref. 22.

[d] After Ref. 26, in which the chosen x and y directions are interchanged with those used here.

[e] ν, β, and γ(CH) are stretching, in-plane, and out-of-plane deformation modes, respectively; ν(CC) and ϕ(CC) are stretching and out-of-plane deformations; α(CCC) is an in-plane deformation, and the X-sensitive modes are all associated with motion of the oxygen atoms: ν, δ, and ν(OH) are, respectively, the stretching, in-plane bending, the out-of-plane (torsional) modes of the OH group, Refs. 15–17, 26.

[f] Shoulder.

TABLE II. IETS data of chemisorbed *p*-X-phenols, where X is F, Cl, Br, and CH_3, on plasma grown Al oxide, i.e., the *p*-substituted phenolate anions.

Vibrational fundamentals in cm^{-1}										
X = F		X = Cl		X = Br		X = CH_3				
IETS[a]	ir-Raman[b]	IETS[a]	ir-Raman[b]	IETS[a]	ir-Raman[b]	IETS[a]	ir-Raman[b]	Symmetry class[c]	Approx. description[d,e]
3040 } (0.50)	3077	3040 (0.30)[f]	3064	3047 (1.10)	3062	3040 (0.35)	3062	ν_1	ν(CH), 1
3040 }	3050	3020 (0.78)	3034	3022 (1.06)[f]	3030	3012 (0.44)	3030	ν_2	ν(CH), 20*a*
1595 (0.35)	1611	1598 (0.85)	1610	1578 (1.15)	1588	1602 (0.39)	1615	ν_3	ν(CC), 8*a*
1504 (0.19)	1512	1491 (0.38)	1494	1487 (0.47)	1498	1565 (0.38)	1515	ν_4	ν(CC), 19*a*
1269 (0.24)	1264	1270 (0.24)	1258	1269 (0.37)	1257	1265 (0.20)	1252	ν_5	ν(CO)
1207 (0.14)	1223	1169 (0.13)	1163	1169 (0.22)	1164	1205 (0.39)	1213	ν_6 } a_1	β(CH), 9*a*
1148 (0.15)	1152	1089 (0.42)	1094	1066 (1.41)	1068	1164 (0.13)	1170	ν_7	X sensitive
1005 (0.10)	1012	1011 (0.34)	1010	1005 (0.55)	1010	1007 (0.13)	1018	ν_8	β(CH), 18*a*
···	852	812 (0.27)	818	814 (0.68)	810	···	843	ν_9	X sensitive
···	747	639 (0.27)	645	610 (0.10)	607	···	738	ν_{10}	X sensitive
···	458	384 (0.19)	379	294 (0.51)	295	461 (0.05)	462	ν_{11}	X sensitive
940 (0.31)	942	951 (0.21)	945	945 (0.32)	945	945 (0.24)	949	ν_{12}	γ(CH), 17*a*
801 (0.51)	809	812 (0.27)	801	814 (0.68)	800	816 (0.25)	810	ν_{13} } a_2	γ(CH), 10*a*
425 (0.50)	390	420 (0.50)	400	418 (0.50)	401	412 (0.50)	407	ν_{14}	ϕ(CC), 16*a*
919 (0.26)	918	931 (0.19)	924	930 (0.32)	926	921 (0.20)	922	ν_{15}	γ(CH), 5
836 (0.26)	829	837 (0.27)	824	834 (0.54)	821	816 (0.25)	817	ν_{16}	γ(CH), 11
701 (0.31)	700	703 (0.67)	696	701 (0.79)	694	701 (0.43)	699	ν_{17}	ϕ(CC), 4
520 (0.52)	507	512 (0.43)	502	512 (0.58)	500	509 (0.47)	507	ν_{18} } b_1	ϕ(CC), 16*b*
375 (0.21)	374	339 (0.19)	325	328 (0.36)	319	312 (0.14)	320	ν_{19}	X sensitive
	175		160		151		178	ν_{20}	X sensitive
3040 } (0.50)	3050	3040		3047		3040	3062	ν_{21}	ν(CH), 20*b*
3040 }	3036	3020		3022		3012	3030	ν_{22}	ν(CH), 7*b*
1595 (0.35)	1605	1598 (0.85)	1592	1578 (1.15)	1588	1602 (0.39)	1598	ν_{23}	ν(CC), 8*b*
1414 (0.25)	1438	1408 (0.19)	1426	1403 (0.10)	1430	1400 (0.19)	1428	ν_{24}	ν(CC), 19*b*
···	1323	···	1318	···	1321	···	1328	ν_{25}	β(CH), 3
1275 (0.10)[f]	1302	1290 (0.10)	1284	1290 (0.12)	1281	1296 (0.11)	1291	ν_{26} } b_2	Kekulé, 14
1088 (0.11)	1089	1089 (0.42)	1109	1101 (0.13)	1092	1095 (0.10)	1109	ν_{27}	β(CH), 15
637 (0.12)	637	589 (0.10)	629	634 (0.32)	632	637 (0.13)	643	ν_{28}	α(CCC), 6*b*
425 (0.50)	445	420 (0.50)	421	418 (0.50)	418	412 (0.50)	426	ν_{29}	X sensitive
···	348	···	265	···	233	335 (0.25)	338	ν_{30}	X sensitive
	3617		3604		3604		3608		ν(OH)
···	1176	···	1172	···	1173	···	1170		δ(OH)
···	283	···	302	···	318	···	306		γ(OH)

[a]As discussed in the text, the relative intensities shown in parentheses are arbitrarily scaled with respect to the line at ≈ 420 cm^{-1} set to unity; where accidental line coincidences are believed to occur, the observed intensity is shared between the coincident modes.

[b]The line position data listed are of the various phenols in dilute solution, Ref. 15.

[c]Considered as having C_{2v} symmetry with the recommended choice of axes, Ref. 22.

[d]ν, β, and γ(CH) are stretching, in-plane, and out-of-plane deformation modes, respectively; ν(CC) and ϕ(CC) are stretching and out-of-plane deformations; α(CCC) is an in-plane deformation, and the X-sensitive modes are all associated with motion of substituent atoms; ν, δ, and γ(OH) are, respectively, the stretching, in-plane bending, the out-of-plane (torsional) modes of the OH groups; description based on the considerations given in Refs. 15, 18, and 21. For examples of the motional complexity of the fundamentals see Refs. 23–25.

[e]The Kekulé mode is a planar ring deformation involving in-phase motion of alternate carbon atom pairs, as suggested by a Kekulé structured six-membered ring, related to the b_{2u} ν_{14} mode of benzene [see E. B. Wilson, Jr., Phys. Rev. **45**, 706 (1934)].

[f]Shoulder.

the number of surface oxide centers immediately adjacent to the OH group with a treatment-dependent distribution of such sites present on the alumina. The precise peak positions observed in the bulk γ-alumina case have been correlated[29] with the acidity of the variously located surface OH groups. The tunnel spectra (including that of an undoped junction) in contrast show a structureless band with a slight asymmetry on its low energy side [see Figs. 2–6], centered at $\simeq 3600$ cm^{-1} with a half-height width of $\simeq 130$ cm^{-1}. Like those on γ alumina, this band shows the expected isotope shift when the surface OH groups are deuterated.[32] If we allow a top electrode shift of 70 cm^{-1} as reported by Kirtley and Hansma, then the band moves to 3670 cm^{-1}. From comparison with the bulk case we conclude that the groups on the plasma grown oxide are of the more acidic type with few or possibly no nearest neighbor oxide anions. Moreover, we have obtained, from a range of primary and secondary amines,[33] high quality tunnel spectra which are consistent with chemisorption via protonation of the amino nitrogen at the oxide surface. Again this reflects the acidity of the surface OH groups. Of

TABLE III. IETS data of chemisorbed *o*- and *m*-X-phenols, where X is Cl and CH_3, in plasma grown Al oxide, i.e., the *o*- and *m*-substituted phenolate anions.

Vibrational fundamentals in cm^{-1}										
X = *o*-Cl		X = *o*-CH_3			X = *m*-Cl		X = *m*-CH_3			
IETS[a]	ir-Raman[b]	IETS[a]	ir-Raman[b]	Approx. description[c]	IETS[a]	ir-Raman[b]	IETS[a]	ir-Raman[b]	Approx. description[c]	Symmetry class[d]
3074 (0.21)	3085	3082 (0.21)						3080		
3042 (1.05)		3050 (0.83)	3060	νCH	3060 (1.73)	3073	3040 (0.46)	3042	νCH	ν_1 ν_2
2986 (0.31)		3003 (0.89)	3028		3017 (0.50)	3057	3007 (1.46)			ν_3 ν_4
1582 (0.66)	1595	1592 (0.82)	1608		1588 (0.86)	1608	1595 (0.66)	1614		ν_5
1560 (0.44)	1584	1575 (0.75)	1587		1568 (0.50)	1599	1580 (0.72)	1600		ν_6
1472 (0.35)	1480	1487 (0.52)	1492	νCC	1481 (0.30)	1489	1484 (0.30)	1490	νCC	ν_7
1439 (0.21)	1461	1461 (0.29)	1462		1424 (0.40)	1462	1454 (0.33)	1462		ν_8
···	1337	···	1324	Kekulé	1297	1310	1308 (0.29)	1306	βCH	ν_9
1279 (0.21)	1294	1300 (0.36)	1300	βCH	1285	1290	···	1281	Kekulé	ν_{10}
1242 (0.19)	1252	1269 (0.35)	1255	X sensitive	1247 (0.30)	1258	1269 (0.34)	1268	X sensitive	ν_{11}
1148 (0.30)	1154	1192 (0.10)	1207	βCH	1154 (0.22)	1154	1161 (0.14)	1163	βCH	ν_{12}
1121 (0.31)	1124	1151 (0.25)	1149	X sensitive	1088 (0.28)	1088	1161 (0.14)	1153[e] 1149	X sensitive	ν_{13} a'
1053 (0.22)	1057	1111 (0.11)	1102	X sensitive	1068 (0.36)	1069	1080 (0.23)	1085[e] 1080	βCH	ν_{14}
1030 (0.31)	1028	1040 (0.10)	1043	βCH	995 (0.26)	998	1000 (0.21)	1000	ring	ν_{15}
844 (0.15)	835	854 (0.39)	842	X sensitive	925 (0.19)	888	935 (0.20)[f]	930	X sensitive	ν_{16}
647 (0.19)	677	761 (0.16)	748	X sensitive	721 (0.15)	687	···	733	X sensitive	ν_{17}
549 (0.48)	557	584 (0.20)	586	X sensitive	584 (0.33)	526	···	536	X sensitive	ν_{18}
···	496	511 (0.10)	529	X sensitive	443 (0.50)	442	519 (0.18)	518	X sensitive	ν_{19}
385 (0.10)	377	420 (0.37)	429	X sensitive	···	410	446 (0.50)	443	X sensitive	ν_{20}
···	250	284 (0.16)	265	X sensitive	254 (0.21)	249	289 (0.10)	297	X sensitive	ν_{21}
960 (0.57)	974	960 (0.36)	967		957 (0.23)	962	955 (0.47)	962		ν_{22}
923 (0.47)	930	930 (0.48)	928		870 (0.20)	885	875 (0.30)[f]	880		ν_{23}
844 (0.15)	846	854 (0.39)	844	γCH	845 (0.20)	859[e] 839	856 (0.55)	855[e] 842	γCH	ν_{24}
751 (0.34)	747	761 (0.16)	749		768 (0.49)	771[e] 765	778 (0.65)	776[e] 767		ν_{25}
713 (0.90)	705	721 (0.82)	711		685 (0.69)	676	695 (0.70)	685		ν_{26} a''
521 (0.10)	528	562 (0.54)	542	ϕCC	584 (0.33)	526	577 (0.63)	560	ϕCC	ν_{27}
443 (1.00)	440	446 (1.00)	442		443 (0.50)	442	446 (0.50)	443		ν_{28}
271 (0.47)	263	284 (0.16)	315	X sensitive	···	233	251 (0.17)	246	X sensitive	ν_{29}
···	174	···	191	X sensitive	···	189	···	211	X sensitive	ν_{30}
	3541		3600	ν(OH)		3593	···	3614	ν(OH)	
···	1196	···	1164	δ(OH)	···	1175[e] 1163	···	1187[e] 1177	δ(OH)	
···	393[e] 361	···	321[e] 297	γ(OH)	···	284[e] 317	···	309[e] 283	γ(OH)	

[a] As discussed in the text, the relative intensities shown in parentheses are arbitrarily scaled with respect to the line at $\simeq 420\ cm^{-1}$ set to unity; where accidental line coincidences are believed to occur, the observed intensity is shared between the coincident modes.

[b] The line position data listed are of the various phenols in dilute solution, Ref. 15.

[c] ν, β, and γ(CH) are stretching, in-plane, and out-of-plane deformation modes, respectively; ν(CC) and ϕ(CC) are stretching and out-of-plane deformations; α(CCC) is an in-plane deformation, and the X-sensitive modes are all associated with motion of substituent atoms; ν, δ, and γ(OH) are, respectively, the stretching, in-plane bending, the out-of-plane (torsional) modes of the OH groups; description based on the considerations given in Refs. 15, 19–21.

[d] Considered as having C_s symmetry with the recommended choice of axes, Ref. 22; a' and a'' are in and out of the molecular plane, respectively.

[e] Doubling of bands due to presence of different rotamers in solution.

[f] Shoulder.

course, the oxide ions proximate to or on the surface will ensure that as in the bulk alumina, the plasma grown oxide is amphoteric.

It should also be noted that no evidence for surface bound molecular water (the expected[34] bands at $\simeq 3300$ and $1650\ cm^{-1}$ are absent) in the doped or undoped oxide

TABLE IV. IETS data, methylgroups vibrations[a] in cm^{-1} of *o*, *m*, and *p*-cresolate anions on Al oxide.

o-Cresolate		*m*-Cresolate		*p*-Cresolate		
IETS	ir-Raman[b]	IETS	ir-Raman[b]	IETS	ir-Raman[b]	Assignment
2939 (0.61)	2974	2956 (0.37)	2980	2914 (0.38)	2970	ν asym
2905 (0.49)	2944	2931 (0.59)	2951	2893 (0.30)	2945	
2855 (0.30)	2916	2850 (0.27)	2924	2868 (0.24)	2922	ν sym
1427 (0.29)	1441	1417 (0.36)	1439	1434 (0.14)	1458	δ asym
	1318	1370 (0.33)	1380	1363 (0.41)	1379	δ sym
1088 (0.24)	1039	1035 (0.10)	1038	1027 (0.23)	1043	Out-of-plane rock
	986	1000 (0.21)	≃1010	977 (0.13)	≃985	In-plane rock

[a]The methyl torsional mode is likely to be below 200 cm^{-1} and hence is omitted.
[b]See Refs. 15 and 21; the *o*- and *m*-compounds have C_s symmetry.

tunnel spectra is ever found. We also conclude from a consideration of the intensity of the OH band in the tunnel spectra that the formation of phenolate ions at the surface with concomitant loss of the phenolic proton does not lead to a buildup of surface OH groups. Such a reaction at the surface may in fact lead, via protonation of surface OH, to the formation of molecular water which is then pumped away during the remainder of the sample preparation to leave the phenolate anion electrostatically bound to cationic aluminium surface centers.

It is also possible for the various phenols to react directly with surface cations; the phenolic proton is then lost to neighboring anionic oxide centers which could react further. Both processes may continue till all reactive sites (i.e., both Brönsted and Lewis acid sites) are used up in the presence of excess of the reactant phenols.

In none of this series of tunnel spectra was there any indication of hydrogen bonded OH groups. All were found to be free of any lines or bands between the CH stretching modes at ≃3000 cm^{-1} and the usual surface OH band at ≃3600 cm^{-1}.

Experiments using phenol deuterated at the OH group and radiolabeled phenol may clarify the surface chemistry involved.

Apart from the OH bands discussed above, the various spectra all show a background band centered at ≃940 cm^{-1} and a much weaker lattice phonon[35] mode at ≃320 cm^{-1}. The former intense band has been variously considered[36,37] as an Al–O stretching mode and/or an Al–O–H bending mode in barrier aluminium oxides and is at least 100 cm^{-1} higher[38] in frequency than the Al–O vibration in the bulk oxide. Recent work using polarized infrared reflection and transmission data obtained from electrolytically grown aluminium oxide films establishes[39] the origin of the band at ≃950 cm^{-1} as the longitudinal component of the Al–O stretching vibration. The corresponding transverse component is found, under transmission only, at ≃650 cm^{-1}. The ≃950 cm^{-1} band is in fact observed when the infrared beam is polarized with the electric vector in the plane of incidence and therefore perpendicular to the oxide surface, i.e., the vibration has its transition moment perpendicular to the surface of the film. In the tunnel junctions such a mode will be readily excited by tunneling electrons. The corresponding transverse component with its transition moment parallel to the surface is not expected to be observed in either the reflection polarized infrared or tunneling experiments, because there can be no electric field adjacent and parallel to a metal surface.

The various tunnel spectra will now be considered in detail.

B. Phenol and *p*-X-substituted derivates (X = F, Cl, Br, and CH_3)

In the case of phenol itself, the various OH bands of the free molecule[15] at 3623, 1175, and 310 cm^{-1}, corresponding to the stretching, in-plane, and out-of-plane bending modes, respectively, are absent from the tunnel spectrum as would be expected from the proposed formation of an adsorbed phenolate anion at the surface. A comparison of the tunnel spectrum of adsorbed phenol reported here (Fig. 2) with that published previously[7] shows a close correspondence apart from possible calibration differences. However, in the present case, the broad band found by Weinberg and co-workers centered at ≃2905 cm^{-1} is absent. We attribute that band to nonphenolic contaminant present in their junction. If the small background OH band already discussed is discounted, we find 22 sharp lines resolved of the 30 ($=3N-6$) fundamental vibrations possible for the 12 ($=N$) atom phenolate system. Of the 25 located below 1610 cm^{-1}, 20 are resolved; the missing five can be accounted for by a shoulder at 1565 cm^{-1} on the intense 1583 cm^{-1} line and by lines at 410, 511, and 949 cm^{-1} which, because of their intensity, we believe to be due to accidental coincidences of the pairs of modes shown in Table I. The tunnel spectrum assignments assume that C_{2v} symmetry is retained at the oxide surface. The five C–H stretching modes expected are located in the two bands of the tunnel spectrum at 2985 and 3036 cm^{-1}. Therefore only one line of the parent phenol system, that at 1339 cm^{-1} ($b_2\nu_{25}$), is not identified in the tunnel spectrum after we allow for the loss of the three OH modes. A corresponding discrepancy is apparent in the phenolate tunnel spectrum of Weinberg *et al.*[7] and in the infrared data of phenol on γ alumina reported by Taylor and Ludlum.[27] The latter have wrongly, we believe, assigned the corresponding liquid state line at 1360 cm^{-1} specifically to the in-plane OH bending mode and in error account for its absence and that of a sup-

posedly coupled vibration at 1474 cm^{-1} in terms of the surface reaction directly. In the present case all but one of the ring C-C stretching modes are found, and if the most recent modifications[15] to the previously accepted assignments[16,17] are correct then the missing mode is that absent C–C ring stretching vibration, located at 1339 cm^{-1} in the parent unassociated phenol. This does have some OH motion involved with it, so not surprisingly it shifts following the surface reaction. As will become apparent subsequently, this same anomaly is a consistent feature of all the tunnel spectra of the phenol adsorbates studied.

From the available infrared and Raman data in monosubstituted benzenes,[26] six of the vibrations present are held to be sensitive to the substituent group and so should show some frequency shift in the phenolate anion since, for example, the 1259 cm^{-1} ($a_1\nu_6$) which is essentially a C–O stretching mode is known to shift to $\simeq$1280 cm^{-1} on going from phenol to aqueous phenolate.[40] The value for this mode which is given as 1286 cm^{-1} by Taylor and Ludlum[27] is here found at 1269 cm^{-1}. It thus shows some of the expected upward shift associated with an increase in the strength of the CO bond in the anion. The same trend is shown by the other X-sensitive vibrations.

Apart from these substituent dependent shifts, the tunnel spectrum positions of the various remaining modes show small shifts which may arise from the expected proximity effects of the top electrode, with CH stretching vibrations affected most. However, some of the shifts are too large to be attributed to the electrode effect alone; this seems particularly true in the four C–C modes ($a_1\nu_4$, $b_2\nu_{23}$, $a_1\nu_5$, and $b_2\nu_{24}$, respectively) at 1583, 1565, 1482, and 1440 cm^{-1}. Since all of these are likely to involve some motion of the phenolate oxygen,[23,24] the shifts found might well reflect changes associated with formation of the anion at the surface.

In common with the tunnel spectrum of the adsorbed phenolate, those of the *p*-substituted compounds show similar spectral changes following adsorption and again, when comparison with the dilute solution vibrational data[15] is made, are consistent with the formation of the corresponding *p*-substituted phenolate anions. The C–O stretching mode in each ($a_1\nu_5$, under the C_{2v} symmetry regime) shows the same shift to higher energy in the anionic species and, as with phenol, the various O–H modes are lost. Again the band ($b_2\nu_{25}$) which is believed to be strongly coupled to the in-plane OH deformation mode at 1328, 1323, 1318, and 1321 cm^{-1} in the parent *p*-cresol, *p*-fluoro, *p*-chloro, and *p*-bromophenol, respectively, is conspicuously absent in the tunnel spectra.

In the tunnel spectrum of *p*-chlorophenolate, 20 lines are resolved of the 26 expected below 1600 cm^{-1}; in the *p*-bromo case, 21 are apparent. Intensity and linewidth considerations suggest that, in both, lines ($a_1\nu_3$ and $b_2\nu_{23}$) are coincident and in each two of the low energy X-sensitive modes ($b_1\nu_{20}$ and $b_2\nu_{30}$) are out of the swept range of the tunnel spectra. One band ($b_2\nu_{25}$) is already accounted for and, as in the unsubstituted phenolate case, that at $\simeq$420 cm^{-1} ($b_2\nu_{29}$) may (allowing for the intensity) be coincident with a line ($a_2\nu_{14}$) close to it at 400 cm^{-1} in the spectrum of the free molecules. In the *p*-chloro case, an additional coincidence is likely at 1089 cm^{-1} ($a_1\nu_7$ and $b_2\nu_{27}$) in view of the observed intensity.

In the *p*-fluorophenolate and the *p*-cresolate spectra (excluding for the present the methyl group vibrations in the latter), two pairs of lines are again held to be accidently coincident; one pair (the $a_1\nu_3$ and $b_2\nu_{23}$ vibrations, weak in the infrared and strong in the Raman spectrum) is close to 1600 cm^{-1} in both. The second coincidence ($a_2\nu_{14}$ and $b_2\nu_{29}$) is located at 425 cm^{-1} and 412 cm^{-1} in the *p*-fluoro and *p*-methyl cases, respectively.

The line expected at $\simeq$350 cm^{-1} ($b_2\nu_{30}$) in the fluoro compound is not observed in the tunnel spectrum; neither are lines at 852, 747, and 458 cm^{-1} ($a_1\nu_9$, ν_{10} and ν_{11}) in the parent phenol. Consideration of the *p*-cresolate spectrum shows that, as with the *p*-fluorophenolate, the lines at 843 and 738 cm^{-1} are not observed and are not accidently coincident with other lines unless their intensity contributions are small. In the *p*-cresol adsorbate the various methyl group modes can be readily identified and are listed in Table IV with the free *p*-cresol methyl group data for comparison. From these it is apparent that the top electrode shifts are largest for the stretching modes, less for the deformations, and least for the rocking motions. The other C–H and C–C stretching vibrations and C–H deformations present show shifts as do those of the *p*-halogenated phenolates which in part will also be due to the upper electrode. It is interesting to note that if the electrode shift found for the CH_3 symmetrical deformation mode is allowed for, then the "corrected" value corresponds almost exactly with that quoted by Taylor and Ludlum[27] for *p*-cresol on bulk alumina.

C. *o*-X-substituted and *m*-X-substituted derivatives (X = Cl and CH_3)

The various possible fundamental vibrations of the *o*- and *m*-substituted phenols, considered under C_s symmetry, split simply into motions in the plane ($21a'$) or perpendicular to the plane ($9a''$) of the molecule if the OH and CH_3 groups are treated as point masses. In the dilute solution vibrational spectra[15] of the *m*-compounds two components are found for certain fundamentals because of the presence of isomers formed by rotation round the C–O bond of the OH group; this also gives a doubling of the OH torsional modes present. The latter effect is also found[15] in the *o*-substituted phenols, and for completeness the relevant line positions are included in Table III. The methyl group modes are in Table IV.

Now, just as in the previous cases, the tunnel spectra are consistent with the formation of phenolate anions with the various OH modes absent in these four spectra. Of the 26 a' and a'' modes below 1620 cm^{-1}, 20 are resolved in the tunnel spectrum of *m*-cresol. Coincidences are believed to arise at 1161 cm^{-1} ($a'\nu_{12}$ and $a'\nu_{13}$) in the adsorbed anion and at 446 cm^{-1} ($a'\nu_{20}$ and $a''\nu_{28}$) in both cases because of the obvious intensi-

ty of these lines. The lines expected at 733 and 536 cm^{-1} ($a'\nu_{17}$ and $a'\nu_{18}$) are not observed; that at 211 cm^{-1} ($a''\nu_{20}$) is again below the swept range. The line at 1281 cm^{-1} which is apparently sensitive to the *m*-substituent in phenols[15] is absent, but since this is likely to be largely C–O stretch in type, it may be moved higher energy and hidden by the other lines present. Since loss of a proton arises when the anion is formed, the doubling of $a'\nu_{13}$, $a'\nu_{14}$, $a''\nu_{24}$, and $a''\nu_{25}$ apparent in the dilute solution spectrum of *m*-cresol is, not surprisingly, lost in the tunnel spectrum.

In the case of *m*-chlorophenolate the line at 410 cm^{-1} ($a'\nu_{20}$) is absent from the tunnel spectrum. The intense line at 584 cm^{-1} may result from a coincidence of $a'\nu_{18}$ and $a''\nu_{27}$, while that at 443 cm^{-1} is probably due to coincidence of $a'\nu_{19}$ and $a''\nu_{28}$. The doubling of $a''\nu_{24}$ and $a''\nu_{25}$ is lost, and $a'\nu_{30}$ is again outside the range covered. All of the lines below 1610 cm^{-1} are therefore accounted for.

There are fewer apparent absences in *o*-substituted compounds. For the *o*-cresolate these are (excluding the methyl group modes) 1324 cm^{-1} ($a'\nu_9$) which is probably the C–O stretching mode and the low energy off-scale line at 191 cm^{-1} ($a''\nu_{30}$). There may be a coincidence for $a'\nu_{21}$ and $a''\nu_{29}$ at 284 cm^{-1}. In the *o*-chlorophenolate case, again the $a'\nu_9$ line at 1337 cm^{-1} in the parent is missing and those at 250 and 174 cm^{-1} ($a'\nu_{21}$ and $a''\nu_{30}$) are outside the swept range. The strong line at 443 cm^{-1} may include both $a'\nu_{19}$ and $a''\nu_{28}$, but otherwise the lines observed correspond well with expectation. The various methyl group modes in the *o*- and *m*-cresol systems are also present in the tunnel spectra and are listed in Table IV.

Although the various stretching modes can be identified, there is some ambiguity about the location of the a' rocking mode in the adsorbed *m*-cresolate; it may be coincident with the $a'\nu_{15}$ fundamental. Otherwise the agreement is good once an allowance for the top electrode shifts is included. Similarly, in the *o*-cresolate the methyl group stretching modes can be identified but the 1318 cm^{-1} symmetric deformation is probably absent as is the a' rocking mode expected at 986 cm^{-1}. While a weak line at 1040 cm^{-1} is present we believe the a'' rocking is also absent since if the *o*-cresolate anion is sited with C–O^- towards the oxide then the CH_3 group adjacent to it will be locked by the proximity of the surface.

D. Adsorbate orientation

We have already argued that the phenols undergo a specific reaction involving the phenolic OH group. The spectral lines are quite narrow and there is little variation in width from line to line. We therefore conclude that apart from the electrostatic interaction with the negatively charged phenolate oxygen the oxide surface has very little effect on the rest of the molecule. Such effects if present would show up as line splitting or broadening in the spectra with some modes being more affected than others. (At the temperature of the measurements there can be no motional averaging.) If this view is correct and the presumed symmetry of the molecule is taken into account, the most reasonable deduction is that the phenolate anions are perpendicular to the oxide surface.

Earlier we saw that the line intensities should have a high dipole orientation dependence. In the C_{2v} systems there is no pronounced difference in intensity of modes associated with motions out of the molecular plane as compared with those in the plane (see Tables I, II, and IV); lines of low or high intensity are, however, found for both types or motion. The same is true for identified stretching and bending modes. Even if the proposed assignments are wrong, these conclusions will still hold. It may seem somewhat surprising that there is not a greater disparity in the relative line intensities associated with the differently classified symmetry types of vibration. If correctly identified, the low intensity of $b_2\nu_{26}$ (e) in the tunnel spectrum is matched by its low intensity in both the infrared and Raman spectra of phenol itself. The strongest line attributed to a single mode is that assigned $b_1\nu_{18}$ (v). It is known to be very strong in the infrared but weak in the Raman spectrum and is in fact an out-of-plane deformation of the carbon skeleton, As such, it has twice the intensity of the $a_1\nu_6$ (q) mode which involves motions of the carbon framework and the oxygen atom and is known to be strong in both the Raman and infrared. For the C_s system it is clear from the data in Tables III and IV that the a'' modes which by symmetry involve motion out of the plane of the adsorbates are rather more intense than those associated with in-plane motion, the a' vibrations. Such is the range of relative intensities within each symmetry class that many lines of comparable intensity occur irrespective of the symmetry of the modes involved. This lack of marked directional dependence can be rationalized in the following terms.

A molecule is not simply an assembly of independent dipoles; coupling between the oscillators ensures that any natural mode of the molecule involves cooperative motions by most of the atoms in the molecule. The interaction of tunneling electrons with such vibrating molecules can take place in a variety of ways and only the presence of a nonzero *z*-axis projection of an oscillating dipole, either permanent or induced, somewhere in the molecule is necessary. In polyatomic adsorbates the complexity of the motion of the various vibration modes will generally ensure the presence of such a *z*-axis component. It is even possible for stretching modes exactly parallel to the oxide to be excited by the tunneling electron because of asymmetries in the electron distribution. Coupling of this type would, however, be expected to lead to weaker lines. We note that the induced dipole need not arise from the polarization by the electric field of the tunneling electron; it may be the result of the applied dc bias or be induced by the presence of the adsorbing surface. Thus almost any motion of the molecule may be excited by the tunneling electron and directional selectivity is largely lost.

An additional important factor in spoiling directional selectivity will be the likely contouring of the upper electrode metal atoms around the organic species; in these circumstances the simple planar model will break

down. There will be, close to the molecule, a range of effective z directions for tunneling, directions which lie at various angles to the principal molecular axis. This would enhance the line intensities of those modes which are inappropriately aligned in terms of the nominal z direction, i.e., parallel to the C_2 axis of the adsorbed simple phenol and p-X substituted phenolates discussed above.

Bogatina *et al.*[11] have reported satisfactory agreement between the observed IET spectrum of benzene in Pb–I–Pb junctions and their predictions based on the assumption that the benzene lies with its plane parallel to the oxide. Our results which are of superior quality would tend to cast doubt on whether conclusions of this certainty can be reached from IET information.

The transition selection rules for a molecule of a given symmetry are rigorous in IET as they are in optical vibrational spectroscopy. In the surface adsorbed situation perturbation of the adsorbate may change the symmetry of the molecule and accordingly the selection rules. Thus comparison of tunnel spectra should correctly be made with those obtained by infrared and Raman techniques on the same adsorbate/adsorbent system rather than with the vibrational behavior of the free molecule directly.

VII. SUMMARY AND CONCLUSIONS

We have vapor doped Al–I–Pb tunnel junctions with a range of phenols. The high resolution spectra obtained have allowed most of the possible molecular modes to be tentatively identified. This gives clear evidence of the presence of phenolate anions due to the reaction of the parent species with the barrier oxide. Shifts due to the top electrode have been taken into account. A directional dependence of the inelastic tunneling process has been suggested by consideration of the imaging of the molecular dipoles and electron fields in the planar top metal electrode. There is no clear evidence in the results presented here of systematic line intensity variation and it is postulated that for these molecules this may be because of the complexity of the motions involved in the vibrational modes. It is also suggested that the contouring of the lead electrode round the adsorbate has the important effect of obscuring the directional sensitivity of the tunneling process. We have attempted to characterize the chemical nature of the oxide and its surface.

If tunneling results can be compared with infrared and Raman data on surface adsorbates using polarized radiation with the electric field vector perpendicular to the oxide surface as, for example, in a grazing incidence geometry, the differences found will most likely give information on the effects of the top electrode and should otherwise show close agreement.

ACKNOWLEDGMENTS

We wish to thank Dr. W. H. Weinberg and Dr. P. K. Hansma for preprints of their work.

*Work supported by Science Research Council.

[1]R. C. Jaklevic and J. Lambe, Phys. Rev. Lett. 17, 1139 (1966).
[2]P. K. Hansma, *Proceedings of 14th International Low Temperature Physics Conference, Otaniemi*, 1975 (North-Holland, Amsterdam, 1975), Vol. 5, p. 264.
[3]J. Klein, A. Léger, M. Belin, D. Défourneau, and M. J. L. Sangster, Phys. Rev. B 7, 2336 (1973).
[4]B. F. Lewis, M. Mosesman, and W. H. Weinberg, Surf. Sci. 41, 142 (1974).
[5]D. G. Walmsley, I. W. W. McMorris, and N. M. D. Brown, Solid State Commun. 16, 663 (1975).
[6]B. F. Lewis, W. M. Bowser, J. L. Horn, Jr., T. Luu, and W. H. Weinberg, J. Vac. Sci. Technol. 11, 262 (1974).
[7]W. H. Weinberg, W. M. Bowser, and B. F. Lewis, Jpn. J. Appl. Phys. Suppl. 2, Pt. 2, 863 (1974).
[8]D. J. Scalapino and S. M. Marcus, Phys. Rev. Lett. 18, 459 (1967).
[9]See, for instance, C. J. H. Schutte, *The Wave Mechanics of Atoms, Molecules and Ions* (Arnold, London, 1968).
[10]J. Lambe and R. C. Jaklevic, Phys. Rev. 165, 821 (1968).
[11]N. I. Bogatina, I. K. Yanson, I. B. Verkin, and A. G. Batrak, Sov. Phys.-JETP 38, 1162 (1974).
[12]P. R. Antoniewicz, Surf. Sci. 52, 703 (1975).
[13]J. R. Kirtley and P. K. Hansma, Phys. Rev. B 12, 531 (1975).
[14]J. Kirtley and P. K. Hansma, Phys. Rev. B 13, 2910 (1976).
[15]J. H. S. Green, D. J. Harrison, and W. Kynaston, Spectrochim. Acta A 27, 2199 (1971).
[16]J. H. S. Green, J. Chem. Soc. 1961, 2236.
[17]J. C. Evans, Spectrochim. Acta 16, 1382 (1960).
[18]J. H. S. Green, Spectrochim. Acta A 26, 1503 (1970).
[19]J. H. S. Green, Spectrochim. Acta A 26, 1913 (1970).
[20]J. H. S. Green, Spectrochim. Acta A 26, 1523 (1970).
[21]G. Varsanyi, *Vibrational Spectra of Benzene Derivatives* (Academic, New York, 1969).
[22]R. S. Mulliken, J. Chem. Phys. 23, 1997 (1955).
[23]J. H. Scherer, Spectrochim. Acta 19, 601 (1963).
[24]J. R. Scherer, Spectrochim. Acta 21, 321 (1965).
[25]J. R. Scherer, Spectrochim. Acta A 24, 747 (1968).
[26]D. H. Whiffen, J. Chem. Soc. 1956, 1350.
[27]D. R. Taylor and K. H. Ludlum, J. Phys. Chem. 76, 2882 (1972).
[28]I. I. Shabalin, E. A. Kiva, Yu. V. Churkin, L. A. Rusanova, and M. F. Mazitov, Kinet. Katal. 15, 1540 (1974).
[29]J. B. Peri, J. Phys. Chem. 69, 211 (1965).
[30]J. B. Peri, J. Phys. Chem. 69, 220 (1965).
[31]A. A. Tsyganenko and V. N. Kilmov, J. Mol. Struct. 19, 579 (1973).
[32]A. L. Geiger, B. S. Chandrasekhar, and J. G. Adler, Phys. Rev. 188, 1130 (1969).
[33]I. W. N. McMorris, D. Phil. thesis, New University of Ulster, 1975.
[34]L. H. Little, *Infrared Spectra of Absorbed Species* (Academic New York, 1966), p. 233; J. B. Peri and R. B. Hannon, J. Phys. Chem. 64, 1526 (1960).
[35]T. T. Chen and J. G. Adler, Solid State Commun. 8, 1965 (1970).
[36]T. Takamura, H. Kihara-Morishita, and U. Moriyama, Thin Solid Films 6, R17 (1970).
[37]M. G. Simonsen, R. V. Coleman, and P. K. Hansma, J. Chem. Phys. 61, 3789 (1974).
[38]A. V. Uvarov, T. V. Antipina, and S. P. Tikhomirova, Zh. Fiz. Khim. 41, 3059 (1967).
[39]A. J. Maeland, R. Rittenhouse, W. Lahar, and P. V. Romano, Thin Solid Films 21, 67 (1974).
[40]S. Pinchas, Spectrochim. Acta A 28, 801 (1970).